Effect of GaN template layer strain on the growth of $In_xGa_{1-x}N$/GaN MQW Light Emitting Diodes

M.C. Johnson, E.D. Bourret-Courchesne*, J. Wu, Z. Liliental-Weber, D.N. Zakharov

Lawrence Berkeley National Laboratory, Materials Sciences Division, 1 Cyclotron Road, MS2R0200, Berkeley, CA 94720-8197, USA

R.J. Jorgenson and T.B. Ng

Oriol Inc., 3390 Viso Court, Santa Clara, CA 95054, USA

D.E. McCready and J.R. Williams

Environmental Molecular Sciences Laboratory, Pacific Northwest National Laboratory, P.O. Box 999, MS K8-93, Richland, WA 99352, USA

*Corresponding author: Edith Bourret-Courchesne, LBNL 1 Cyclotron Road, MS2R0200, Berkeley, CA 94720-8197, USA (510)486-5553 Fax (510) 486-5530 email EDBourret@lbl.gov

Abstract

GaN template layer strain effects were investigated on the growth of InGaN/GaN LED devices. Seven period InGaN/GaN multiple quantum well structures were deposited on 5µm and 15µm GaN template layers. It was found that the electroluminescence emission of the 15µm device was red-shifted by approximately 132meV. Triple-axis X-Ray Diffraction and Cross-Sectional Transmission Electron Microscopy show that the 15µm templay layer device was virtually unstrained while the 5µm layer experienced tensile strain. Dynamic Secondary Ion Mass Spectrometry depth profiles show that the 15µm template layer device had an average indium concentration of 11% higher than that of the 5µm template layer device even though the structures were deposited during the same growth run. It was also found that the 15µm layer device had a higher growth rate than the 5µm template layer device. This difference in indium concentration and growth rate was due to changes in thermodynamic limitations caused by strain differences in the template layers.

I. INTRODUCTION

Group-III nitride materials have become extremely important in device applications over the last decade. High-brightness light emitting diodes (LEDs) and high-power laser diodes (LDs) based on these materials are already commercially available. With the emergence of white LEDs [1], high-density memory devices [2], and high-power microelectronics [3], a more fundamental understanding of Group III-nitride device performance is needed. This information is especially critical for the design and fabrication of advanced devices that include ternary and quaternary alloys. There has been a variety of research into the physical, chemical, and optical properties of InGaN/GaN multilayer quantum well (MQW) structures used for LEDs and LDs [4-9]. The active regions in such devices are known to behave differently due to physical and electronic variations in the InGaN/GaN quantum well, but a fundamental understanding of the mechanisms that determine emission characteristics is lacking. This is due in large part to the complexity of typical InGaN/GaN MQW structures and the difficulties of incorporating In to form the InGaN ternary alloy. There exists a large body of literature describing the apparent roles that composition and phase segregation [4,5], thickness [6], strain [7,8], and structure [9] have on optical properties. However, the intrinsic effects of these phenomena on device properties and performance remain relatively poorly defined.

Group-III nitrides cannot be economically fabricated in bulk single-crystal form due to a large excess dissociation pressure at the high temperatures necessary for crystal growth. For commercial applications, these materials must be deposited heteroepitaxially on a foreign substrate. For example, InGaN/GaN MQWs are typically grown atop a thick GaN template layer deposited on a sapphire substrate. However, GaN has large lattice

and thermal expansion coefficient mismatches with sapphire, approximately 32% and 56% respectively. These factors induce relatively high strain in the GaN template, which in turn causes the propagation of dislocations. The strain in the GaN template and the resulting dislocations affect the properties of the overlaying MQW structure.

In the case of GaN deposited on sapphire <001> using MOCVD, Detchprohm *et al.* [10,11] described the relationship between the perpendicular lattice parameter (*c*) and layer thickness. In that study, the perpendicular lattice parameter decreased rapidly from the substrate-film interface toward the sample surface across several tens of microns of layer thickness. Above ~20 μm, *c* decreased more slowly, and at ~150 μm, the value of *c* equilibrated. It could be inferred that a significantly less thick GaN template underlying an InGaN/GaN MQW structure is typically highly strained. In addition, residual strain in the template could strain the entire device, especially in the InGaN active regions that do not exceed the critical thickness for strain relaxation [12].

Several groups have shown that strain in the InGaN/GaN MQW regions cause emission shift due to electronic effects [7,8,13]. Group III-Nitrides have large piezoelectric constants in the <001> direction. Strain in these layers is believed to increase this piezoelectric field which tilts the potential profile and results in a red-shift of the optical emission, known as the Quantum Confined Stark Effect (QCSE).

It has also been shown that alloy composition can fluctuate in the well layers due to strain [14-16]. Thermodynamic analysis shows that the lattice constraint from substrate materials influences the thermodynamic properties of the subsequent epilayers [15,17]. Koukitu *et al.* [18] suggest that the most likely reason for these thermodynamic changes is a limited solubility of In in GaN due to the big difference of the In-N and Ga-

N bond length. As a result, strain can have a large influence on the In incorporation in the $In_xGa_{1-x}N$ layers during growth because of the resulting lattice parameters of the "substrate" material (GaN template layer). The strains produced by the difference in the lattice parameters and the thermal expansion coefficients between hetereoepitaxial materials are commonly known to be deposited pseudomorphically. But if strain is too great, the film accomodates this thermodynamic barrier by forming defects and/or three dimensional growth [12,19]. Therefore, the amount and type of strain (tensile or compressive) can affect the growth mechanism of InGaN on GaN.

In this study, we examine the effects of template strain on $In_xGa_{1-x}N$/GaN MQW LED structures grown by Metallorganic Chemical Vapor Deposition (MOCVD). Seven period $In_xGa_{1-x}N$/GaN structures were grown at the same time on GaN templates of two different thickness. All growth parameters were identical for the two samples, with the GaN template thickness being the only difference. Surprisingly, this resulted in the samples having emission outputs with a 132 meV difference in peak energies. In this paper, we show that GaN template layer strain (thickness) plays a major role in $In_xGa_{1-x}N$ growth mechanism by altering In incorporation in the growing films. Triple-axis X-ray diffraction (TAXRD) shows an inverse relationship between layer thickness and strain in the GaN template layer. Transmission electron microscopy (TEM) confirmed the expected proportional relationship between template thickness and dislocation density. Dynamic Secondary Ion Mass Spectrometry (SIMS) depth profiling shows an average indium concentration difference of 11% between the samples.

II. EXPERIMENT

A. Film Growth

Two InGaN/GaN MQW LEDs were grown on 2-inch diameter <001> sapphire substrates using a vertical flow EMCORE D180 MOCVD multiwafer reactor. Figure 1 shows a schematic cross-section of the two devices. In one of the devices, the GaN template was 5 μm thick; in the other it was 15 μm thick. Trimethylgallium (TMG), trimethylindium (TMI), ammonia, silane, and biscyclopentadienyl magnesium were used as precursors for Ga, In, N, Si, and Mg, respectively. To facilitate the incorporation of indium, N_2 was used as the carrier and dilution gases during deposition of the active InGaN/GaN regions. H_2 was used for all other layers. A thin GaN nucleation layer was deposited on the substrate at 550°C, followed by growth of the thick Si-doped, n-type GaN template layer at 1050°C. The deposition temperature of the overlaying seven-period InGaN/GaN MQW structure (30 Å /170 Å) was 780°C, followed by the Mg-doped, p-type AlGaN electron blocking layer and the Mg-doped, p-type GaN cap. It is important to note that these structures were grown at the same time.

B. Characterization

The LED structures were examined by triple-axis X-ray diffraction (TAXRD) to determine the thickness of the layers and the strain in the GaN templates. The specimens were aligned on, and normalized to, the (006) reflection of the sapphire substrate at Ω = 20.8400°, 2θ = 41.680° for the TAXRD measurements. Cross-section transmission electron microscopy (XTEM) was used to confirm the thickness data from TAXRD and to measure the dislocation densities in the templates. Room temperature (RT)

electroluminescence was used for optical characterization. Finally, dynamic SIMS was used to obtain a concentration profile for the quantum wells. The TAXRD data were collected using a Philips X'Pert Pro MRD system (PW3040/60 type) with a Cu X-ray source operated at 1.8 kW. The incident beam conditioner was hybrid-type that combined an X-ray mirror with a four-bounce Ge (220) crystal monochromator. The diffracted beam conditioner was a three-bounce Ge (220) analyzer crystal. The XTEM thin sections were examined using a Jeol 200CX transmission electron microscope. The electroluminescence emission was generated with a constant current source to the device using a HP3245A Universal Source power supply. The emission was dispersed with a 1 m double-grating monochromator and measured using a Hamamatsu R928 photomultiplier tube. Dynamic SIMS depth profiling was performed using a Cameca Magnetic Sector Secondary Ion Mass-Spectrometer at MAS, INC. located in Sunnyvale, CA. Duoplasmatron and surface ionization Cs source was used to sputter the sample surface producing ionized secondary particles. The secondary ion extraction system and beam forming system (immersion lens) directs the beam to an electrostatic analyzer to provide energy filtering and the magnetic sector analyzer to provide mass separation of the secondary ions. The intensity of this mass-separated image was then measured and recorded.

III. RESULTS AND DISCUSSION

Figure 2 shows the resulting electroluminescence (EL) for the devices. It is shown that there is a large shift in device emission although the structures were grown simultaneously in a multiwafer reactor.

Figure 3 shows the experimental and fitted TAXRD rocking curves for both LEDs. The many and well resolved satellite peaks indicate these were high-quality InGaN/GaN MQW structures. The program Bede RADS Mercury v3.88 was used to fit the experimental TAXRD rocking curves. This program utilizes dynamic theory in its calculations. The principal objective of fitting the experimental TAXRD rocking curve data was determination of the thickness of the layers above the templates. Because this program limits fitting and dynamic simulation to one set of Miller indices, the sapphire (006) reflections were ignored, and the (002) reflections from the GaN template layers were treated as the substrate in both sample models. Table 1 is a summary of the properties which shows the layer thickness data obtained from these fitting exercises. The two devices were of similar structure where the fitted thickness of the active InGaN wells were approximately 30 Å. The fitted thickness of the barrier, blocking, and capping layers were significantly different, but the thickness variation of these inactive layers are not expected to contribute to device performance or optical properties.

The superlattice period thickness obtained from fitting (195 Å for the 5μm template, and 200 Å for the 15μm template) was confirmed by direct calculation using the program Philips X'Pert Epitaxy 4.0. The positions of four of the superlattice fringes on the low-angle side of GaN (002) were determined manually, and the period thickness (t) was calculated by

$$\Delta\Omega = \lambda \sin \varepsilon / t \sin 2\theta, \qquad (1)$$

where λ is the wavelength (1.5406 Å), ε is the angle between the diffracted beam and the sample surface (equal to the average value of 2θ minus Ω for adjacent fringes), 2θ is the average value of 2θ for adjacent fringes, and ΔΩ is the separation of adjacent fringes in radians. The results from these direction calculations agreed with those from fitting within ±1 Å. As discussed below, the TAXRD thickness data were also confirmed by XTEM.

Figure 4 shows an expanded-scale overlay plot of the TAXRD rocking curves from both LEDs. Note the position difference for GaN (002) and the coincidence of sapphire (006) in the inset. The variant position of GaN (002) against the substrate reference implied a strain difference in the template layers. The GaN (002) peak positions were determined by gaussian profile fitting using the program Jade 6.5 (Materials Data Inc., Livermore, CA). The corresponding value of *c* was 5.1874 Å for the 5μm template, and 5.1854 Å for the 15μm template. These data were used to calculate perpendicular strain (ε_{zz}) using

$$\varepsilon_{zz} = (c\text{-}c_o)/c_o, \tag{2}$$

where c_o = 5.1855 Å is the lattice parameter of bulk, unstrained GaN [10]. The calculated strain was +0.04% in the 5μm template and -0.002% in the 15μm template device. Parallel strain calculations were performed using

$$\varepsilon_{xx} = (a\text{-}a_o)/a_o, \tag{3}$$

where a_o = 3.1891 Å. The in-plane lattice constant a was determined from the profile-fitted position of the asymmetric (105) reflection. This gave a parallel strain of –0.10% for the 5µm template layer and +0.009% for the 15µm template layer. From this it would appear there was virtually no residual strain in the thicker template, while significantly more was present in the thinner template. These results are in agreement with those of Detchprohm [10,11]. Figure 4 also shows that the 1st-order superlattice fringe is displaced toward relatively higher angle for the 5µm template layer device. This result is consistent with higher strain in the superlattice structure atop the 5µm template.

Figure 5 shows a XTEM image of the MQW region for each device. XTEM was used to determine the barrier thickness to be 165 Å and 170 Å for the 5µm and 15µm template layer devices, respectively. The thickness of the quantum wells was more difficult to measure but appears to be approximately 25 Å and 30 Å for the 5µm and 15µm template layer devices, respectively. These data are in agreement with the TAXRD results. Additionally, the capping layer is much thicker for the 15µm template layer device than that of the 5µm layer device. Therefore the 15µm layer device had a higher growth rate than the 5µm device. Since both devices were grown simultaneously, the total thickness of the wells, barriers, and capping layers should have been equal.

Figure 6 verifies the thickness of the template layers to be 5µm and 15µm. More importantly, the edge dislocation density was 0.4×10^8 cm^{-2} and 1.9×10^8 cm^{-2} for the 5µm and 15µm template layer devices, respectively. The thicker template has a dislocation density about 5 times that of the thinner template. This result is consistent with the strain relaxation observed in the 15µm device via TAXRD.

It is proposed that the strain relaxation in the 15μm template resulted from the formation of these dislocations. S.E. Park *et al.* [12] found that the strains in a thicker layer begin to relax, generating defects such as dislocations and three-dimensional growth. The increase in dislocation density relieves strain caused by lattice and thermal mismatch between GaN and sapphire. Relief of this strain via dislocation formation results in a decrease of the *c* lattice parameter, as seen in the TAXRD data, resulting in an almost unstrained template layer.

Dynamic SIMS depth profiling was performed to obtain concentration data for the device active region. Absolute values for the In concentration could not be resolved due to the wells being very thin. On a relative scale, the average In concentration was approximately 11% higher for the 15μm sample. This higher In concentration is consistent with the lower energy EL emission for the 15μm layer device shown in Figure 2. Using the standard equation determined by Wu *et al.*[20]

$$Eg = 0.77x + 3.42(1-x) – 1.43x(1-x), \quad (4)$$

the relative In concentrations were calculated from the peak maxima in Figure 2 to be approximately x = 0.23 for the 5μm template layer device and x =0.26 for the 15μm template layer device. This method gives a relative In concentration difference of approximately 12%. This is within the experimental error of the value of 11% obtained by SIMS analysis. Although these samples were grown at the same time and should be identical in structure and composition, it is shown that the emission shift between these devices is due to a difference in In concentration.

This concentration difference is attributed to a strain induced thermodynamic effect that influenced layer growth. TAXRD shows that there is a strain difference between the GaN template layers with the 5μm template layer having more tensile strain with the 15μm template layer being virtually unstrained. Gorgens *et al*. [14] clearly show that a fully relaxed sample is able to incorporate more indium during growth than a strained sample. They attribute this to a pseudomorphic growth mode on GaN. Additionally, we have shown that the less strained 15μm template sample has a higher growth rate than the strained 5μm template sample. It is well known that an increased growth rate for $In_xGa_{1-x}N$ increases the amount of In incorporation due to less time for the In to be able to desorb and therefore are trapped by the growing layer [21,22]. It is clearly advantageous to use a relaxed GaN template layer for growing InGaN/GaN MQW structures so that the emission output can be predicted and consistently produced. The strain relieved by formation of dislocations in the thick template layer also allows growth of a smooth cap layer.

IV. CONCLUSION

$In_xGa_{1-x}N$/GaN MQW structures were grown at the same time using GaN template layer thickness of 5μm and 15μm. The electroluminescence emission was found to be redshifted by 132 meV for the 15μm template layer device. TAXRD and XTEM were used to characterize the template layers and it was found that the 15μm template layer was virtually unstrained while the 5μm template layer device exhibited a relatively large tensile strain. Dynamic SIMS depth profiling was performed to obtain a relative In concentration difference of 11% with the 15μm sample having a higher In concentration. This is consistent with the EL emission results. Additionally, it was

found that the growth rate was increased for the 15μm template sample. This difference in indium incorporation and growth rate was assigned to changes in thermodynamic limitations caused by differences in strain of the "substrate" layers. Therefore, it is very important to take template layer strain into consideration when depositing InGaN/GaN MQW. It also implies that it is advantageous to use a less strained template layer to be able to incorporate higher indium contents.

ACKNOWLEDGEMENTS

This work was supported by the Director, Office of Science, Office of Basic Energy Sciences, Division of Materials Science and Engineering, of the U.S. Department of Energy under Contract No. DE-AC03-76SF00098. The research described in this paper was performed in part in the Environmental Molecular Sciences Laboratory, a national scientific user facility sponsored by the US Department of Energy's Office of Biological and Environmental Research and located at Pacific Northwest National Laboratory in Richland, WA. The authors would like to thank D. Kouzminov at MAS, Inc. for SIMS depth profiling measurements and analysis.

References

1. Y.L. Li, Th. Gessman, E.F. Schubert, and J.K. Sheu, J. Appl. Phys. **94**, 2167 (2003).

2. T. Ohno, S. Ito, T. Kawakami, And M. Taneya, Appl. Phys. Letts. **83**, 1098 (2003).

3. J. Lee, D.M. Liu, Z.J. Lin, W. Lu, J.S. Flynn, and G.R. Brandes, Solid State Elect. **47,** 2081 (2003).

4. A. Hangleiter, F. Hitzel, S. Lahmann, and U. Rossow, Appl. Phys. Lett. **83**, 1169 (2003)

5. I. Ho, and G.B. Stringfellow, Appl. Phys. Lett. **69**, 2701 (1996).

6. F. Shulze, J. Blasing, A. Dadgar, and A. Krost, Appl. Phys. Lett. **82**, 4558 (2003).

7. J. Bai, T. Wang, and S. Sakai, J. Appl. Phys. **90**, 1740 (2001).

8. S. Pereira, M.R. Correia, E. Pereira, E. Alves, A.D. Sequeira, and N. Franco, Appl. Phys. Lett. **79**, 1432 (2001).

9. F. Sholz, J. Off, A. Kniest, L. Gorgens, and O. Ambacher, Mat. Sci. & Eng. B **B59**, 268 (1999).

10. T. Detchprohm, K. Hiramatsu, K. Itoh, and I. Akasaki, Jpn. J. Appl. Phys. **31**, L1454 (1992).

11. K. Hiramatsu, T. Detchprohm, and I. Akasaki, Jpn. J. Appl. Phys. **32**, L1528 (1993).

12. S.E. Park, O. Byungsung, C.R. Lee, J. Crystal Growth **249**, 455 (2003).

13. M.E. Aumer, S.F. LeBoeuf, S.M. Bedair, M. Smith, J.Y. Lin, and H.X. Jiang, Appl. Phys. Lett. **77**, 821 (2000).

14. L. Gorgens, O. Ambacher, M. Stutzmann, C. Miskys, F. Scholz, and J. Off, Appl. Phys. Lett. **76**, 577 (1999).

15. Y. Kanagawa, T. Ito, Y. Kumagai, A. Koukitu, and N. Kawaguchi, Jpn. J. Appl. Phys. **42**, L95 (2003).

16. Y. Kawaguchi, M. Shimizu, K. Hiramatsu, and N. Sawaki, Mater. Res. Soc. Symp. Proc. **449**, (1997).

17. A. Koukitu, N. Takahashi, T. Taki, H. Seki, Jpn. J. Appl. Phys. **35**, L673 (1996).

18. A. Koukitu and H. Seki, Second International Conference on Nitride Semiconductor, ICNS, Tokushima, Japan, 1997.

19. C.A. Parker, J.C. Roberts, S.M. Bedair, M.J. Reed, S.X. Liu, and N.A. El-Masry, Appl. Phys. Lett. **75**, 2776 (1999).

20. J. Wu, W. Walukiewicz, K.M. Yu, J.W. Ager III, E.E. Haller, H. Lu, W.J. Schaff, Appl. Phys. Lett. **80**, 4741(2002).

21. S. Keller and S.P. DenBaars, J. Crystal Growth, **248**, 479 (2003).

22. S. Keller, B.P. Keller, D. Kapolnek, A.C. Abare, H. Masui, L.A. Coldren, U.K. Mishra, and S.P. DenBaars, Appl. Phys. Lett. **68**, 3147 (1996).

Figure and Table Captions

Table 1 – Comparison of physical and optical properties of two LEDs grown simultaneously on different thickness of GaN template layers. It is important to note that these devices were grown at the same time and would expect to have the same thickness and concentrations for the active and capping layers.

Figure 1 – Schematic of LED device structure. It is important to note that the InGaN/GaN MQWs and capping layers were grown at the same time on a different thickness (5 or 15 μm) of GaN template layer.

Figure 2 – EL emission for the same LED device grown simultaneously on different thickness (5 or 15 μm) GaN template layers. It is shown that the thick template layer device is red-shifted by approximately 132 meV.

Figure 3 – Measured and fitted high resolution TAXRD patterns for InGaN/GaN MQW structures on (002) ω-2θ mode.

Figure 4 – Expanded scale overlay of the (002) GaN peak obtained using ω-2θ mode for both devices. The inset shows the coincidence of the sapphire (006) peak.

Figure 5 – XTEM image of each device. The growth rate is larger for the 15μm template layer device as determined by the thicker layers for the same growth times. Also, notice the uniform MQWs and the smooth capping layer for the 15μm device.

Figure 6 – XTEM comparison of each device to show the difference in template layer thickness. The 15μm template has a dislocation density of 1.9×10^{8} cm^{-2} while the 5μm template has a dislocation density of 0.4×10^{8} cm^{-2}.

Table 1

Layer	**QW098**	**QW061**
p-GaN Capping Layer	1200 Å	1015 Å
p-AlGaN Blocking Layer	175 Å	195 Å
GaN Barrier	165 Å	170 Å
InGaN Well	30 Å	30 Å
GaN template	**5µm**	**15µm**
Property		
EL emission output (eV)	2.57	2.44
%perpendicular strain	+0.04%	-0.002%
%parallel strain	-0.10%	+0.009%
Dislocation density (#/cm^2)	0.4x10^8	1.9x10^8
[In] difference via SIMS (%)	N/A	11% higher

Figure 1

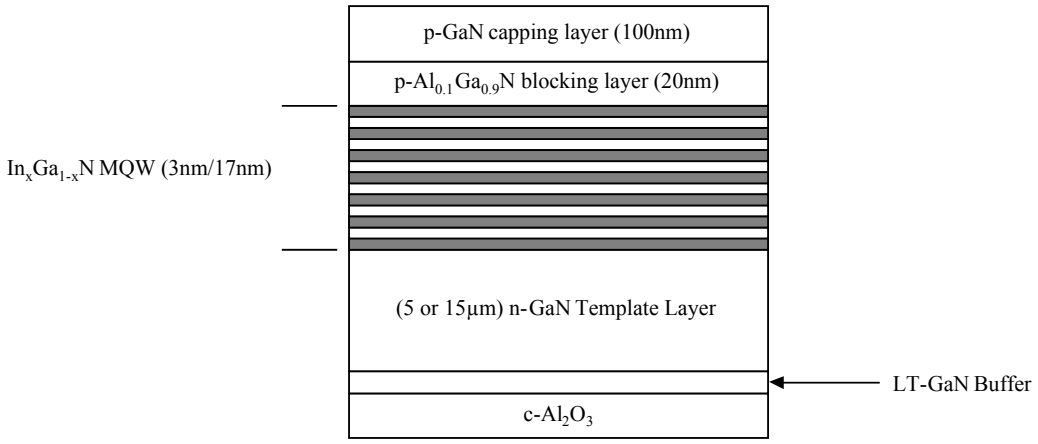
p-GaN capping layer (100nm)
p-Al0.1Ga0.9N blocking layer (20nm)
InxGa1-xN MQW (3nm/17nm)
(5 or 15μm) n-GaN Template Layer
LT-GaN Buffer
c-Al2O3

Figure 2

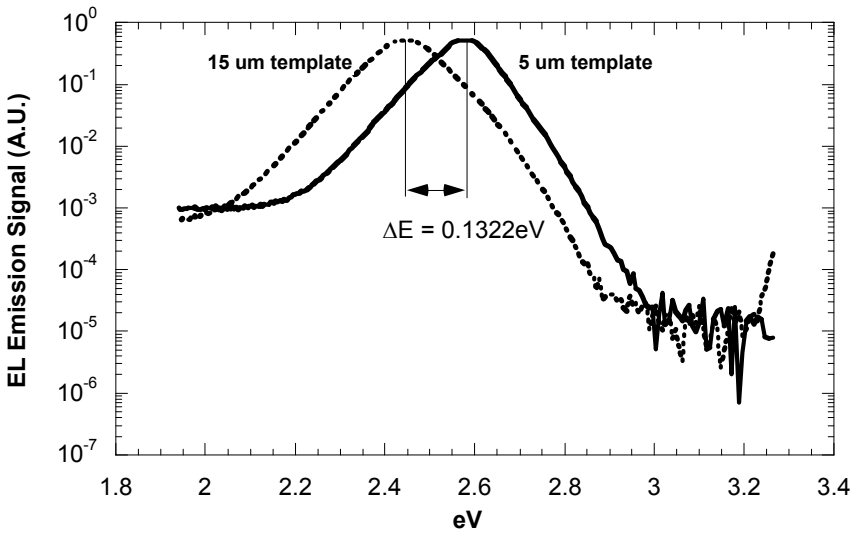
EL Emission Signal (A.U.)
10^0
10^-1
10^-2
10^-3
10^-4
10^-5
10^-6
10^-7
15 um template
5 um template
ΔE = 0.1322eV
1.8
2
2.2
2.4
2.6
2.8
3
3.2
3.4
eV

Figure 3

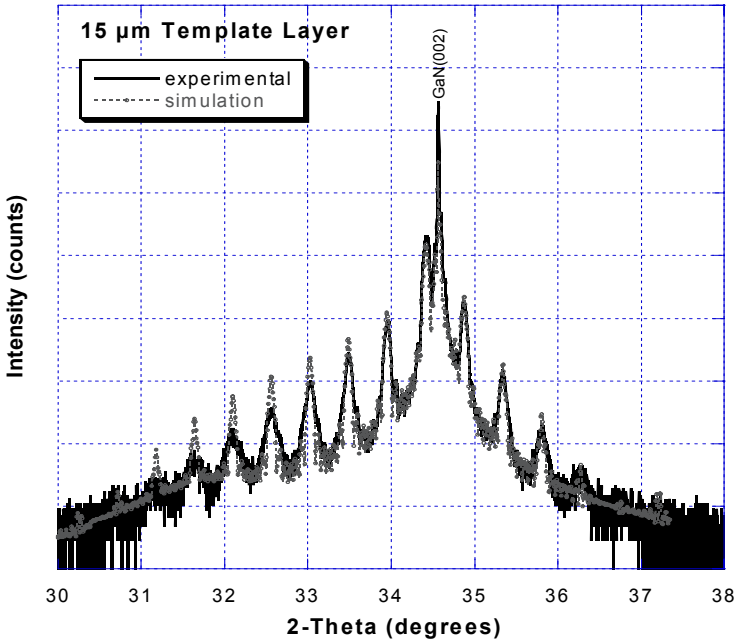
15 µm Template Layer
experimental
simulation
GaN(002)
Intensity (counts)
30
31
32
33
34
35
36
37
38
2-Theta (degrees)

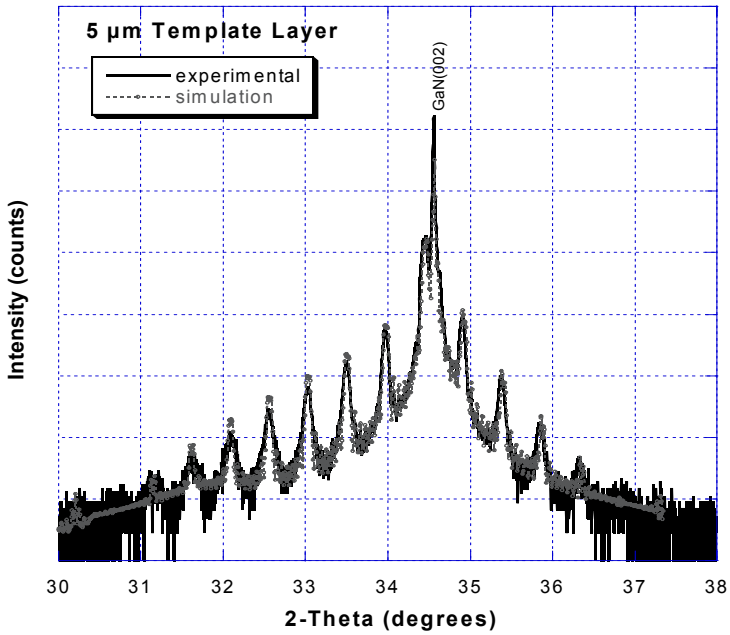
5 µm Template Layer
experimental
simulation
GaN(002)
Intensity (counts)
30
31
32
33
34
35
36
37
38
2-Theta (degrees)

Figure 4

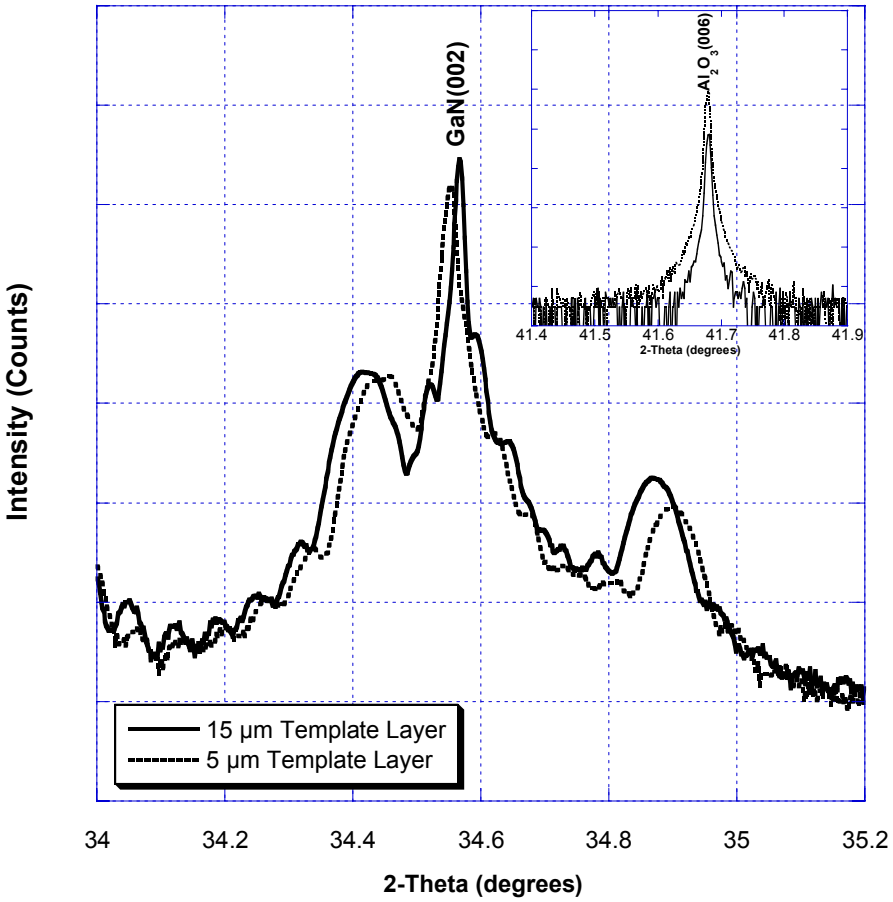
GaN(002)
Al2O3(006)
41.4
41.5
41.6
41.7
41.8
41.9
2-Theta (degrees)
15 µm Template Layer
5 µm Template Layer
Intensity (Counts)
34
34.2
34.4
34.6
34.8
35
35.2
2-Theta (degrees)

Figure 5

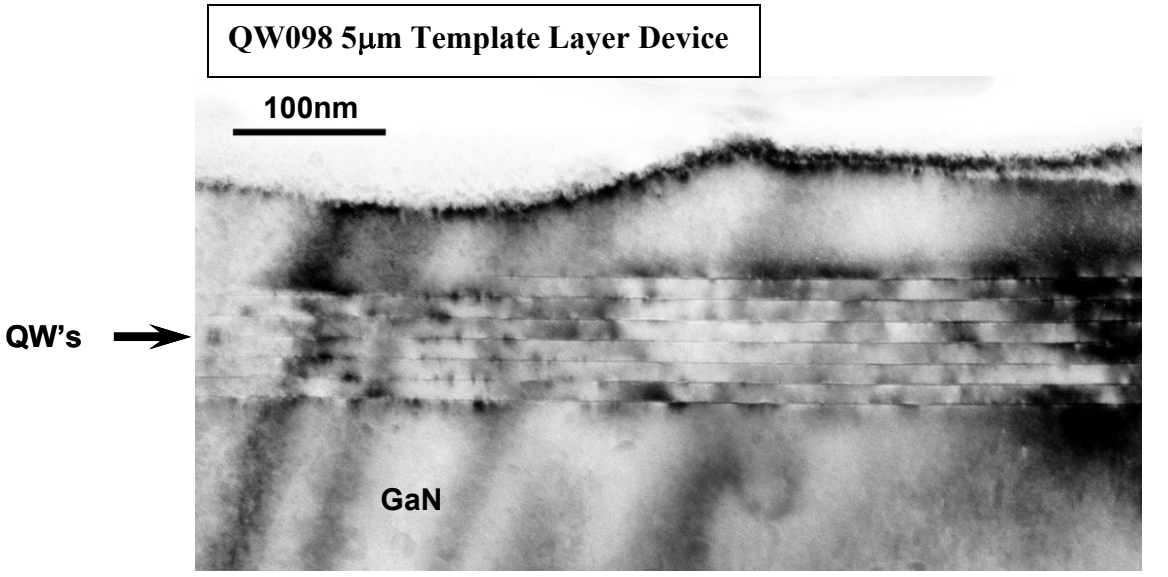
QW098 5μm Template Layer Device
100nm
QW's
GaN

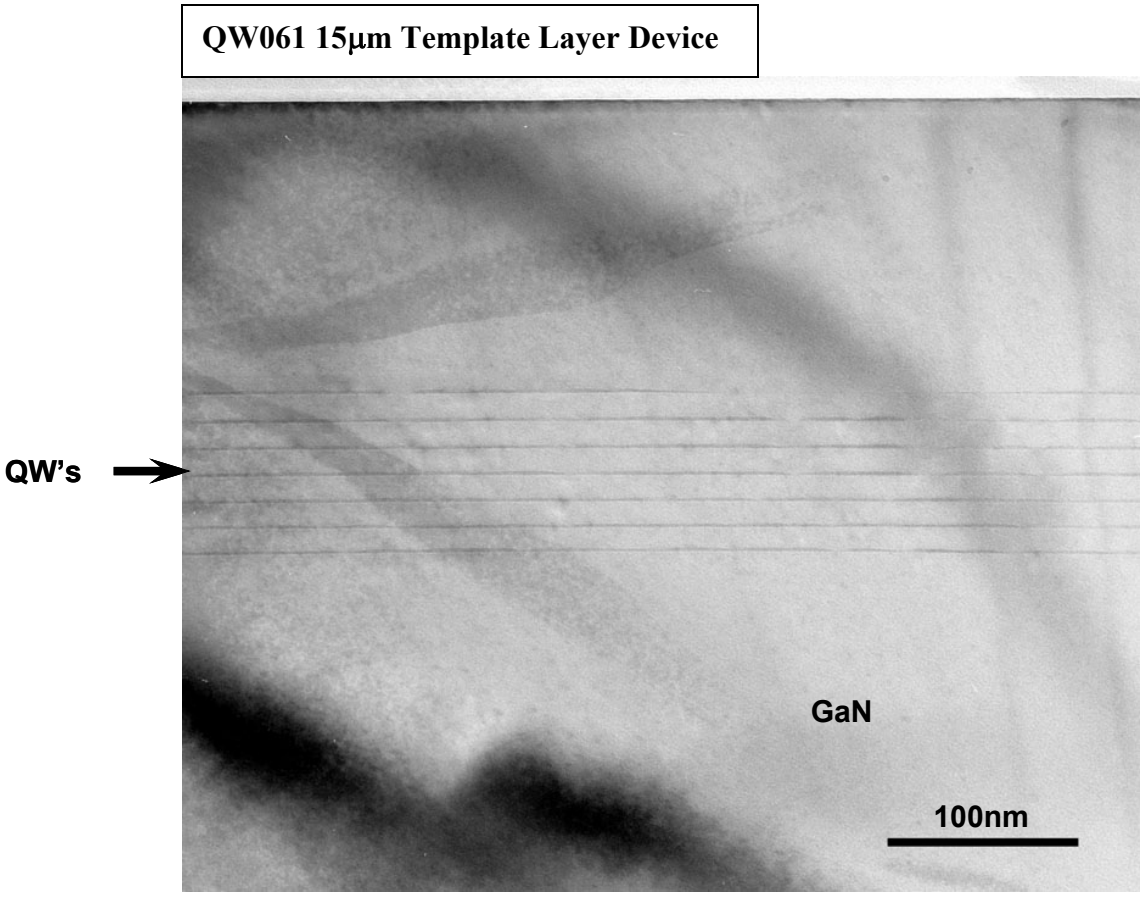
QW061 15μm Template Layer Device
QW's
GaN
100nm

Figure 6

QW061 15μm Template Layer

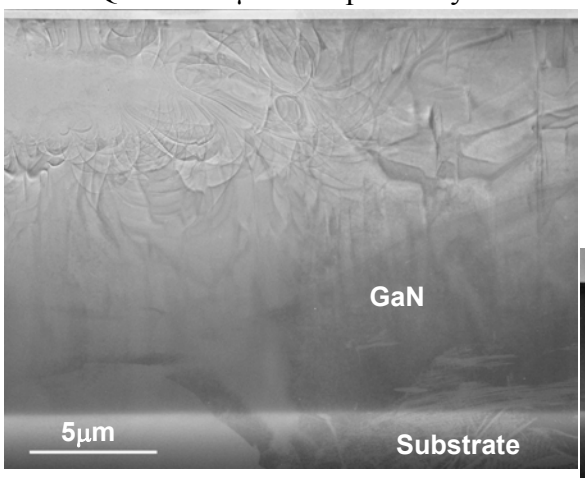

QW098 5μm Template Layer